# Effect of particle size distribution on flowability of granulated lactose

AUTHOR(S):

Kudo, Yozo; Yasuda, Masatoshi; Matsusaka, Shuji

CITATION:

Kudo, Yozo ...[et al]. Effect of particle size distribution on flowability of granulated lactose. Advanced Powder Technology 2019, 31(1): 121-127

ISSUE DATE:

2019-01

URL:

http://hdl.handle.net/2433/250978

Advanced Powder Technology 31 (2020) 121–127

Contents lists available at ScienceDirect

Advanced Powder Technology

journal homepage: www.elsevier.com/locate/apt

Original Research Paper

# Effect of particle size distribution on flowability of granulated lactose

Yozo Kudo, Masatoshi Yasuda, Shuji Matsusaka *

*Department of Chemical Engineering, Kyoto University, Kyoto 615-8510, Japan*

ARTICLE INFO

*Article history:*
Received 21 August 2019
Received in revised form 27 September 2019
Accepted 2 October 2019
Available online 24 October 2019

*Keywords:*
Flowability
Granule
Lactose
Particle size distribution
Friction property

ABSTRACT

The flowability of powders used in tableting significantly affects tablet weight and content uniformity of active pharmaceutical ingredients. Use of granulated materials instead of powdered materials can improve flowability. In this study, the effect of particle size distribution on flowability of granulated lactose was quantitatively analyzed. Three types of granulated lactose were classified into progressively narrower size fractions, and nine samples were systematically prepared. The mass median diameters were nearly constant (i.e., 130.5 ± 13.5 μm) and the geometric standard deviations ranged from 1.29 to 2.04. Two flow properties (angle of repose and compressibility) were measured. The correlations between flow properties and the particle size distributions were analyzed, and the coefficients of determination were obtained for different particle diameters and cumulative mass fractions. The optimal conditions to maximize the coefficients of determination were defined. Furthermore, static and dynamic friction properties were evaluated, and their correlations with particle size distribution were calculated.


## 1. Introduction

Excipients are critical to optimal tablet performance. However, inappropriate combinations of excipients and active pharmaceutical ingredients (API) can result in decreased powder flowability, which can affect tablet weight and API content uniformity [1]. Lactose is widely used as an excipient because of its excellent physical and chemical stability, low hygroscopicity, water solubility, and cost effectiveness [2].

Conventional methods such as measurement of the angle of repose and compressibility have been used to evaluate powder flowability in pharmaceutical tableting [3,4]. However, due to improvements in tablet design using direct compaction, alternative methods for characterizing powder flowability are required.

Shear cell tests are used to evaluate the mechanical properties of consolidated powders, such as yield locus, critical state line, angle of friction, shear cohesion, and flow function, which are determined from measurements conducted during shear and normal stress conditions [5]. Rotating drum tests can be used to evaluate aggregation properties, which are based on avalanching behavior observed at various rotation speeds and operation times [6]. Powder rheology tests measure the forces acting on blades rotating in a powder bed or a fluidized bed [7]. The vibrating tube method [8–10] and the vibration shear tube method [11,12] measure the mass of powder discharged from the tube as a function of vibration intensity, which is used to analyze the differences between static and dynamic friction properties. The decision to use a particular test method depends on its applicability, purpose, and conditions of the powder [13–15].

Previous studies have shown that addition of a small amount of fine particles can improve powder flowability, which was dependent on mixing time and intensity [16,17]. Due to the presence of fine particles on the surfaces, the apparent contact distance is increased, resulting in reduced adhesion forces [18]. This mechanism is similar to that caused by surface roughness [19–21].

Recently, APIs have been fabricated with increasingly smaller particle diameters to enhance dissolution [22]. Consequently, powder handling has become more difficult. Even when surfaces are covered with fine particles, improvements in flowability are minimal. To solve this problem, granulated materials have been used instead of powdered materials [23,24].

Many factors influence powder flowability, such as particle size, shape, density, adhesiveness, electrostatic chargeability, and other surface conditions of the particles. In particular, particle size and shape are the most important factors for flowability. The effect of particle size and shape on the flowability of consolidated powder beds has been evaluated using shear cell tests [25]. The effect of these physical properties on flowability of lactose has been evaluated using several methods [26,27]. The flowability of microcrystalline cellulose with different aspect ratios was examined using the vibration shear tube method [12]. Powdered, granulated,

* Corresponding author.
*E-mail address:* matsu@cheme.kyoto-u.ac.jp (S. Matsusaka).

https://doi.org/10.1016/j.apt.2019.10.004
0921-8831/

and spray-dried mannitol have been characterized using two flowability testers [28]. Comparative evaluation of flow properties of granules has been conducted [29].

Powder flowability depends on the distribution and the average values of the physical properties of formulations. However, methods to quantitatively evaluate the correlation between flowability and distributions of physical properties have not been developed.

In this study, the effects of distributions of physical properties on flowability of granulated lactose were quantitatively evaluated. Nine samples were systematically prepared by classifying three types of granulated lactose into progressively narrower size fractions. Two flow properties (angle of repose and compressibility) of each sample were measured, and the correlation between the flow properties and the distributions of the physical properties were analyzed in detail. In addition, static and dynamic friction properties were evaluated.

## 2. Materials and methods

### 2.1. Materials

Granulated lactose, Dilactose® R (Freund), SuperTab® 30GR (DFE Pharma), and Tablettose® 80 (Meggle) were used as excipients in this study.

Fig. 1 shows images of granules collected using a scanning electron microscope (SEM, VE-9800, Keyence Corporation). The three types of granulated lactose are designated as lactose A, B, and C. The images indicate that the granules had rough surfaces and the particle shapes were irregular. However, the aspect ratios were not too large. In addition, these samples had broad size distributions. In particular, lactose B and C contained more small particles than lactose A.

### 2.2. Preparation of samples and measurement of particle size and shape

To analyze the effect of particle size distribution on flowability, the granules were classified into progressively narrowing size fractions. Large granules were removed using a 212 μm sieve, and small granules were removed using a 75 μm sieve or an air classifier (TC-15, Nisshin Engineering). Nine samples were systematically prepared. The particle size distribution of each sample was measured using a laser diffraction particle size analyzer (SALD-2200, Shimadzu).

Particle shape was quantified using a particle image analyzer (Morphologi G3, Malvern Instruments). The granules were dispersed on a plate using airflow with a gauge pressure of 0.1 MPa. The granules were photographed digitally at a magnification of 247× with a pixel size of 0.56 μm. To analyze particle shape, we quantified circularity ($C_{ir}$), which can be used to quantitatively evaluate particle shape irregularities such as surface roughness, as determined by the following equation,

$$C_{ir} = \frac{2\sqrt{\pi A}}{P} \quad (1)$$

where $A$ is the particle area and $P$ is the particle perimeter.

### 2.3. Evaluation of flowability

We measured the angle of repose ($\phi$) and compressibility ($C$). The $\phi$ values were measured using a device (AOR-57, Tsutsui Scientific Instruments) designed for this purpose. Each sample was discharged from a hole with an inner diameter of 8 mm and, while maintaining a free fall distance of 50 ± 5 mm, accumulated on a disk 60 mm in diameter. Compressibility values were determined using a tap density tester (TPM-1, Tsutsui Scientific Instruments) as follows. First, a 150-ml graduated cylinder was loosely filled with 100 ml of sample and the bulk density ($\rho_b$) was measured. Next, the cylinder containing the sample was tapped from a height of 20 mm 200 times at intervals of 2 s, allowing for measurement of the tapped density ($\rho_t$). The $C$ value was determined using the following equation:

$$C = \frac{\rho_t - \rho_b}{\rho_t} \quad (2)$$

We also characterized flowability using the vibrating tube method to evaluate the static and dynamic friction properties of the samples. The amounts of granules discharged from a tip was

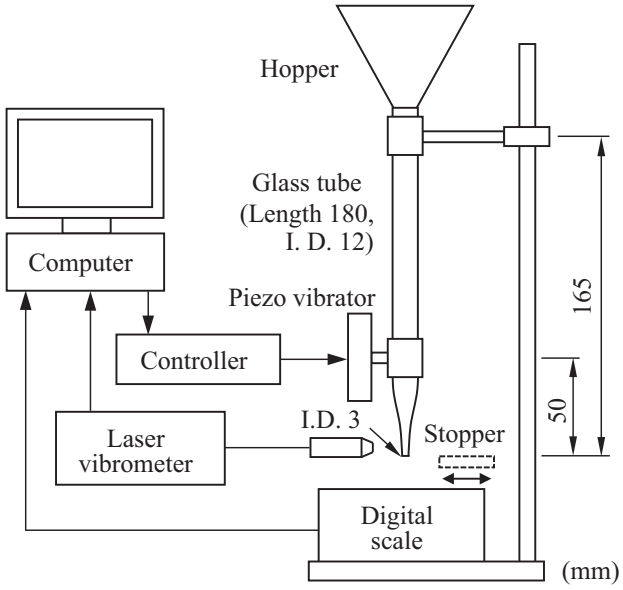


**Fig. 2.** Schematic diagram of the vibrating tube system.

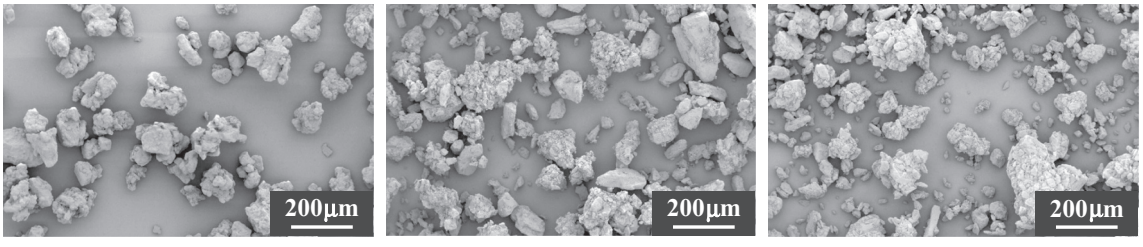


(a) Lactose A (b) Lactose B (c) Lactose C

**Fig. 1.** SEM images of granules.

measured at different vibration conditions. This method enables high-sensitivity measurement of powder flowability, and requires a small amount of sample [8–10].

Fig. 2 shows a schematic diagram of the experimental apparatus for the vibrating tube method. This system is based on the Dynamic Powder Flow Tester® (IMP Co., Ltd.), which consists of a glass tube, a piezoelectric vibrator, a laser vibrometer, a digital scale, and a computer. The length and inner diameter of the glass tube were 180 and 12 mm, respectively. The inner diameter of the tip was narrowed to 3 mm to increase the discharge resistance. The vibration frequency was set to 340 Hz, and the amplitude of vibration was increased for 60 s at a constant rate. The flowability profile, reported as the relationship between the mass flow rate and the vibration acceleration, was obtained.

All experiments were conducted under standard laboratory conditions (temperature: 25 ± 2 °C, relative humidity: 50 ± 10%), and minor environmental variations did not affect the experimental results.

## 3. Results and discussion

### 3.1. Particle size and shape distribution

Fig. 3 shows the mass-based particle size distributions of each of the samples. These measurements indicated that the particle size distributions were classified by narrowing ranges. To quantify the width of the distribution, the geometric standard deviation ($\sigma_{gDp}$) was calculated as follows:

$$\sigma_{gDp} = \frac{D_{p50}}{D_{p15.9}} \tag{3}$$

where $D_{p50}$ is the mass median diameter and $D_{p15.9}$ is the particle diameter at 15.9% of the sample mass. The three $D_{p50}$ values for lactose A were in the range of 141.5 ± 2.5 μm, and the value of $\sigma_{gDp}$ decreased from 1.41 to 1.29 by applying the above classification. The $D_{p50}$ values for lactose B and C were 135.0 ± 5.0 μm and 124.0 ± 7.0 μm, respectively, and the $\sigma_{gDp}$ decreased in a manner similar to that of lactose A. All particle size distribution results are summarized in Table 1.

Fig. 4 shows projection images of lactose A1, arranged in increasing order of circularity, obtained using a particle image analyzer. The particle diameters in these images were 141 μm, which was equal to the $D_{p50}$ value. As circularity increased, particle shape irregularity and surface roughness decreased.

Fig. 5 shows the particle shape distributions of each sample, as measured using a particle image analyzer. The symbols in this figure are defined in Table 1. To quantify the widths of the distributions, we used the geometric standard deviation ($\sigma_{gCir}$) using the following equation:

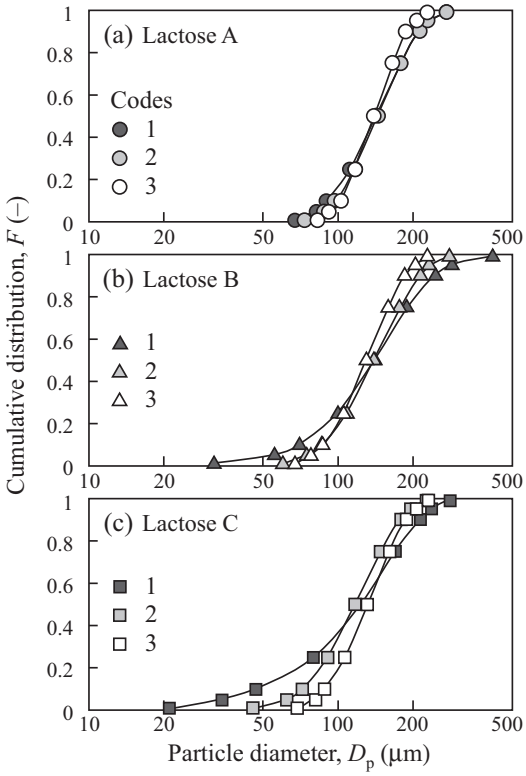


**Fig. 3.** Particle size distributions measured using laser diffraction.

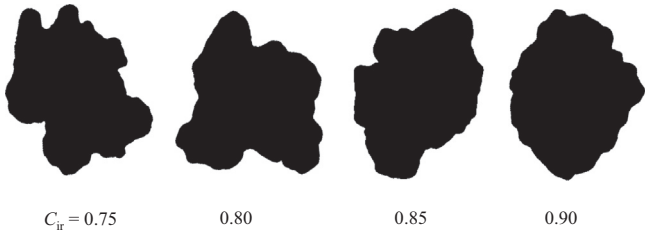


**Fig. 4.** Projection images of lactose A1, and circularities obtained using a particle image analyzer.

$$\sigma_{gCir} = \frac{C_{ir50}}{C_{ir15.9}} \tag{4}$$

where $C_{ir50}$ is the median circularity and $C_{ir15.9}$ is the circularity at 15.9% of the particles. The $C_{ir50}$ values for all of the samples ranged

**Table 1**
Physical properties of samples.

| Material | Code | Symbol | $D_{p10}$ (μm) | $D_{p50}$ (μm) | $\sigma_{gDp}$ (–) | $C_{ir50}$ (–) | $\sigma_{gCir}$ (–) |
|---|---|---|---|---|---|---|---|
| Lactose A | A-1 | ● | 90 | 141 | 1.41 | 0.85 | 1.08 |
| | A-2 | ● | 97 | 144 | 1.37 | 0.83 | 1.07 |
| | A-3 | ○ | 102 | 139 | 1.29 | 0.88 | 1.06 |
| Lactose B | B-1 | ▲ | 70 | 140 | 1.68 | 0.86 | 1.11 |
| | B-2 | △ | 86 | 139 | 1.45 | 0.81 | 1.10 |
| | B-3 | △ | 86 | 130 | 1.38 | 0.88 | 1.08 |
| Lactose C | C-1 | ■ | 47 | 123 | 2.04 | 0.90 | 1.08 |
| | C-2 | ■ | 72 | 117 | 1.44 | 0.89 | 1.07 |
| | C-3 | □ | 88 | 131 | 1.37 | 0.87 | 1.07 |

$D_{p10}$: particle diameter at 10% of the sample mass; $D_{p50}$: mass median particle diameter.
$\sigma_{gDp}$: geometric standard deviation of particle diameter; $C_{ir50}$: count median circularity.
$\sigma_{gCir}$: geometric standard deviation of circularity.

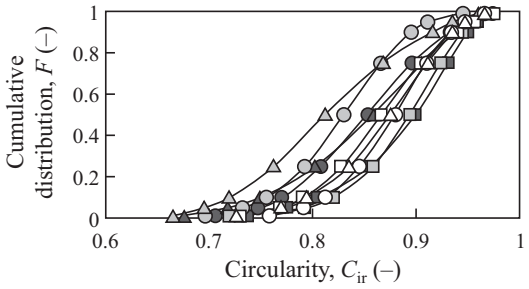


**Fig. 5.** Particle shape distributions measured using a particle image analyzer.

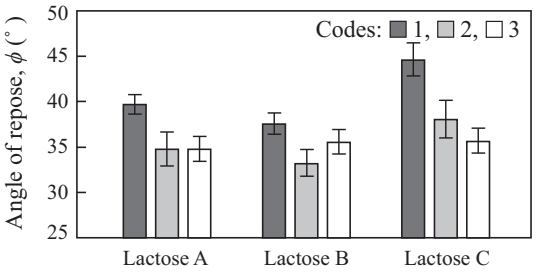


**Fig. 6.** Results of angle of repose.

from 0.81 to 0.90, and the $\sigma_{gCir}$ values ranged from 1.06 to 1.11. All circularity results are summarized in Table 1.

### 3.2. Angle of repose and compressibility

Fig. 6 shows a bar chart representing the angle of repose $\phi$ results obtained from the nine samples. The results for each type of granulated lactose are arranged in descending order of width of particle size distribution. Sample codes in this figure correspond to those in Table 1. Each value represents the mean of three independent experiments and the error bars indicate standard deviations. The $\phi$ value of lactose A1 was 40°, and the values of A2 and A3, which had narrower particle size distributions, were relatively lower. A similar tendency was observed for lactose B and C. In particular, the $\phi$ value for lactose C clearly decreased with decreasing particle size distribution.

Fig. 7(a) shows the effect of the particle diameter at 10% of the sample mass ($D_{p10}$) on $\phi$ for each the samples. The symbols in this figure are defined in Table 1. The value of $\phi$ decreased with increases in $D_{p10}$ (negative correlation). These results indicated that reduction of the proportion of the number of particles with diameters smaller than 100 μm improved flowability. The coefficient of determination ($R^2$) produced by linear regression analysis was 0.65. Fig. 7(b) shows the effect of the $D_{p50}$ on the $\phi$ value. A similar negative correlation was observed between these two variables. However, the $R^2$ value was as low as 0.22, which was significantly lower than that observed for the $D_{p10}$ values. These results indicated that the average value of the particle size distribution was not suitable for evaluating the effect of particle size on flowability. As such, the effect of the cumulative mass fraction ($F_{Dp}$) on $R^2$ must be evaluated.

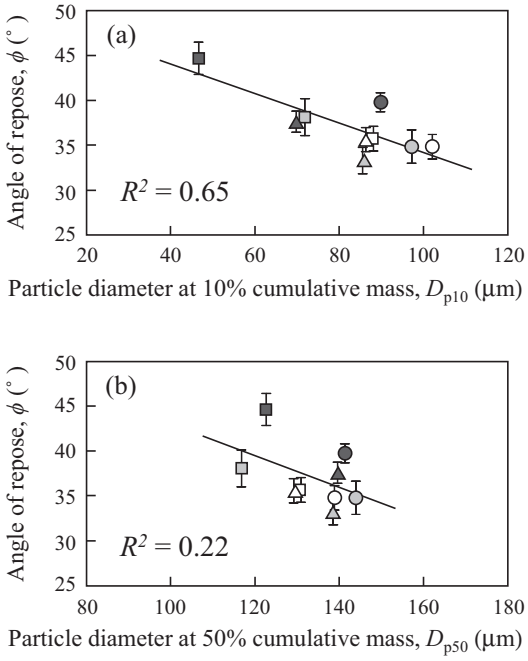


**Fig. 7.** Effects of particle diameter at 10% and 50% of cumulative mass on angle of repose.

Fig. 8 shows the $R^2$ value for the relationship between the angle of repose and $F_{Dp}$. As $F_{Dp}$ increased, the $R^2$ value increased, and reached a maximum at $F_{Dp} = 0.1$. As $F_{Dp}$ increased above 0.1, the $R^2$ value decreased. These results were likely due to two factors: (1) when $F_{Dp}$ was very small, the amount of data was limited; (2) when $F_{Dp}$ was large, the data included large particles and small particles. In previous studies, $D_{p10}$, $D_{p50}$, $D_{p90}$, and the differences between these values, were used to evaluate the effects of particle size distribution on powder flowability [15,28,29]. In our quantitative analysis, the validity of $D_{p10}$ as an indicator of powder flowability was confirmed. As such, the analysis methods in this study may be beneficial for evaluation of the effects of particle size distribution on flowability.

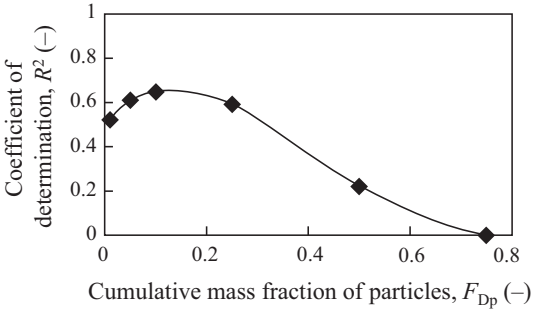


**Fig. 8.** $R^2$ value for the relationship between $\phi$ and $F_{Dp}$.

Fig. 9 summarizes the compressibility results. For each of the types of granulated lactose, the compressibility clearly decreased with decreasing width of particle size distribution.

Fig. 10(a), which summarizes the effects of $D_{p10}$ on $C$, demonstrates a clear negative correlation between the two variables, with $R^2$ values as high as 0.92. Therefore, the proportion of small particles less than 100 μm was the main factor that influenced compressibility. Fig. 10(b) shows the effect of $D_{p50}$ on $C$. A similar negative correlation to that observed between $C$ and $D_{P50}$ was observed between these two variables. However, the $R^2$ value for the relationship between $C$ and $D_{P50}$ was 0.41, which was significantly lower than that for $D_{p10}$.

Fig. 11 shows the $R^2$ value for the relationship between $C$ and $F_{Dp}$. The results for $C$ were similar to those for angle of repose in that the $R^2$ value was maximal at $F_{Dp} = 0.1$. The maximum $R^2$ value was 0.92, which indicated that the particle size distribution affected the compressibility more significantly than it affected

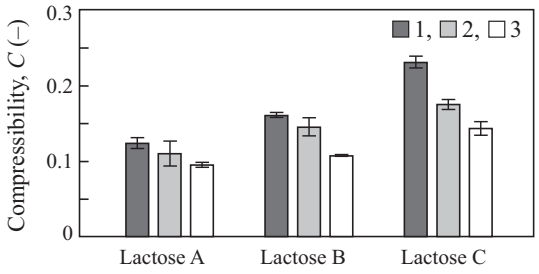


**Fig. 9.** Results of compressibility.

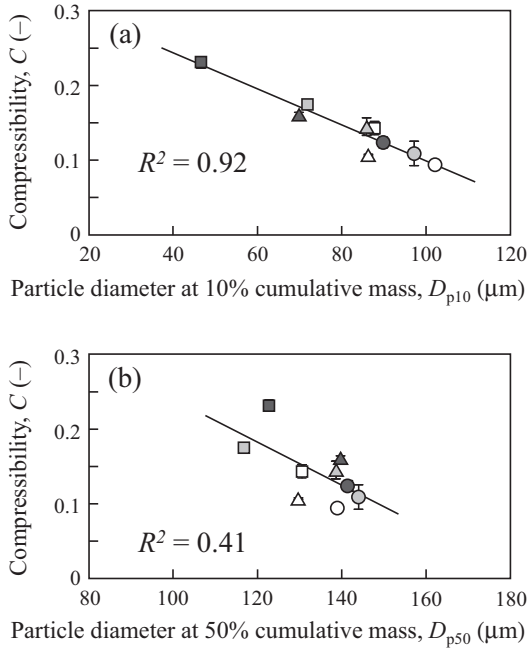


**Fig. 10.** Effects of particle diameter at 10% and 50% of cumulative mass on compressibility.

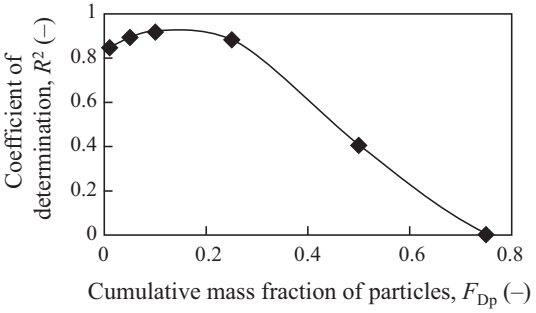


**Fig. 11.** $R^2$ value for the relationship between $C$ and $F_{Dp}$.

the angle of repose. The evaluation method with high correlation is considered to have fewer factors, and reduction of the proportion of small particles will be an effective method to improve the compressibility.

The above analysis method was also used to evaluate the effects of particle shape distribution on flowability. However, no clear correlation was observed, and the shape of the granules had little effect at $C_{ir50}$ = 0.81–0.90 and $\sigma_{gCir}$ = 1.06–1.11. These results were likely due to the samples being prepared by particle size classification. If the samples had been prepared based on particle shape distribution, the effect of particle shape may have been significant. Although many reports have discussed the effects of particle size and shape distributions, the results always depend on the nature of the samples [26–29]. Therefore, appropriate analysis methods to evaluate physical property distributions are required. The method presented in this study, in which the relationship between $R^2$ and $F_{Dp}$ was evaluated, will provide objective and appropriate evidence that can be used to develop materials in the pharmaceutical field and to optimize granulation conditions in formulation development.

### 3.3. Vibrating tube method

Although angle of repose and compressibility are properties indicative of powder flowability, these flow properties are influenced by various factors including static and dynamic friction. We evaluated the static and dynamic friction properties of lactose granules using the vibrating tube method.

Fig. 12 shows representative results of the flowability profiles obtained using the vibrating tube method. The three results are arranged in descending order of the widths of the particle size distributions. Each flowability profile represents the mean of seven independent experiments and the error bars indicate standard deviations. Although the flowability profiles depended on particle size distribution, these profiles had some features in common. The granules became fluidized as the vibration accelerated, allowing the granules to flow out of the glass tube. As the vibration continued to accelerate, the state of fluidization was enhanced, and the mass flow rate increased, allowing for a high degree of flowability. However, once the vibration accelerated to a greater extent, the granules became compressed, and the mass flow rate decreased slightly.

Flowability is related to static friction at the vibrational acceleration at which the granules begin to flow, which is termed the critical vibration acceleration ($\alpha_c$). Smaller $\alpha_c$ values indicate higher flowability. Each $\alpha_c$ value was determined as the value of the $x$-axis intercept, which was obtained from the linear approximation of the sharp increase in mass flow rate [16,17].

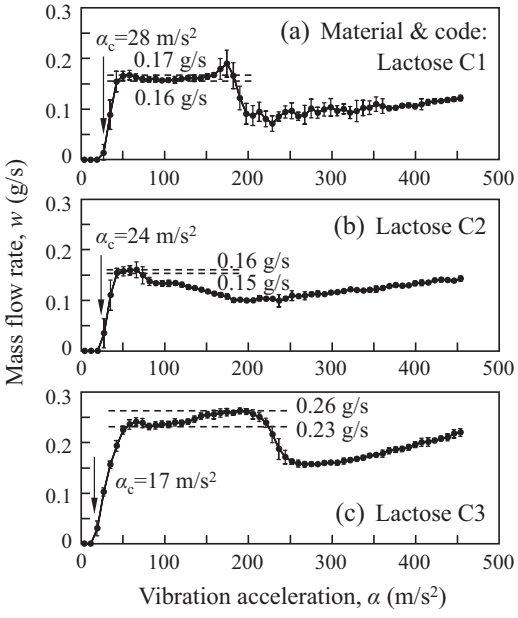


**Fig. 12.** Flowability profiles obtained using the vibrating tube method ($\alpha_c$: critical vibration acceleration).

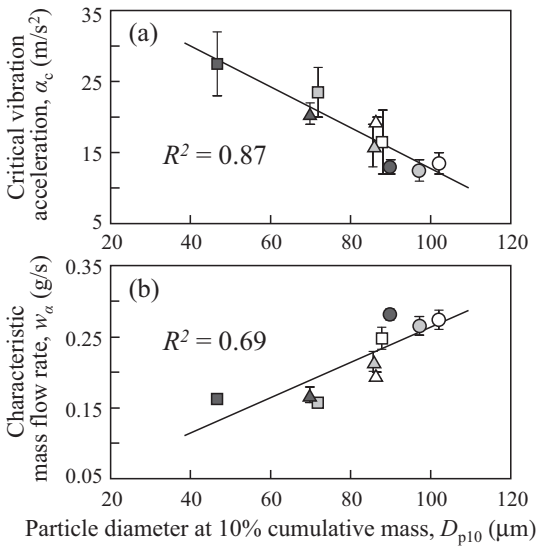


**Fig. 13.** Effect of particle diameter at 10% of cumulative mass on (a) critical vibration acceleration and (b) characteristic mass flow rate.

Flowability related to dynamic friction was evaluated using the mass flow rate ($w_\alpha$) at the stable flow region after the sharp increase in mass flow rate. Since the load applied during measurement of the angle of repose and compressibility was not excessively large, we evaluated the flowability using the vibrating tube method, and we analyzed the data at low vibrational acceleration.

For lactose C1, the two values obtained were $\alpha_c = 28$ m/s$^2$ and $w_\alpha = 0.16$–$0.17$ g/s. For lactose C3, which had a low proportion of small particles, $\alpha_c$ decreased to 17 m/s$^2$ and $w_\alpha$ increased to 0.23–0.26 g/s. These results suggested that the flowability related to the static and dynamic friction increased with a decreased proportion of small particles.

Fig. 13(a) shows the effect of $D_{p10}$ on $\alpha_c$ for each of the samples. The error bars indicate maximum and minimum values of $\alpha_c$ obtained from seven independent experiments, and the symbols are defined in Table 1. The $\alpha_c$ and $D_{p10}$ values were negatively correlated. The coefficient of determination for this relationship was high ($R^2 = 0.87$), which suggested that removal of small particles was an effective method to improve flowability related to static friction.

Fig. 13(b) shows a positive correlation between $w_\alpha$ and $D_{p10}$. The coefficient of determination for this relationship was 0.69, which was slightly lower than that observed for static friction. Thus, dynamic friction is considered to have more factors, and the proportion of small particles is one of the main factors. These results indicated that removal of small particles was an effective strategy to improve flowability related to dynamic friction.

## 4. Summary and conclusion

In the present study, three types of granulated lactose were classified into progressively narrower size fractions, and nine samples with mass median diameters of 130.5 ± 13.5 μm and different geometric standard deviations ranging from 1.29 to 2.04 were prepared to evaluate the flowability of granules. Three different tests were conducted to determine flow properties (the angle of repose, compressibility, and static and dynamic friction). These properties were evaluated by focusing on the distributions of physical properties (particle size and shape). The results obtained from the experiments performed in this study are summarized as follows: The relationships between flow properties and particle diameter were obtained, and the coefficients of determination $R^2$ of the associated linear regression analyses were determined for ranges of $D_p$ and $F_{Dp}$. The maximum $R^2$ values were obtained at $F_{Dp} = 0.1$. The maximum $R^2$ value for compressibility was 0.92, which was larger than that for the angle of repose. The distributions of granule circularity were measured, and the medians and the geometric standard deviations were distributed across the ranges of 0.81–0.90 and 1.06–1.11, respectively. The dependence of flow properties on particle shape was minimal. Static and dynamic friction were determined using the vibrating tube method. The $R^2$ value for flowability related to static friction at $F_{Dp} = 0.1$ was 0.87, which was larger than that for dynamic friction. The method presented in this study for evaluating the relationship between $R^2$ and $F_{Dp}$, provided objective and appropriate evidence.

## References

[1] Y. Takeuchi, E. Katsuno, S. Yajima, T. Tomita, K. Tahara, H. Takeuchi, Evaluation of some excipients during direct tableting processes using their flowability index and shearing test, J. Soc. Powder Technol. Jpn. 51 (2014) 77–87.
[2] M.C. Gohel, P.D. Jogani, A review of co-processed directly compressible excipients, J. Pharm. Pharmaceut. Sci. 8 (2005) 76–93.
[3] R.L. Carr, Evaluating flow properties of solids, Chem. Eng. (January 18) (1965) 163–168.
[4] The Japanese Pharmacopoeia Seventeenth Edition, The ministry of health, labour and welfare (2016) 2425–2426.
[5] E. Guerin, P. Tchoreloff, B. Leclerc, D. Tanguy, M. Deleuil, G. Couarraze, Rheological characterization of pharmaceutical powders using tap testing, shear cell and mercury porosimeter, Int. J. Pharm. 189 (1999) 91–103.
[6] A.W. Alexander, B. Chaudhuri, A. Faqih, F.J. Muzzio, C. Davies, M.S. Tomassone, Avalanching flow of cohesive powders, Powder Technol. 164 (2006) 13–21.
[7] M. Leturia, M. Benali, S. Lagarde, I. Ronga, K. Saleh, Characterization of flow properties of cohesive powders: a comparative study of traditional and new testing methods, Powder Technol. 253 (2014) 406–423.
[8] Y. Jiang, S. Matsusaka, H. Masuda, T. Yokoyama, Evaluation of flowability of composite particles and powder mixtures by a vibrating capillary method, J. Chem. Eng. Jpn. 39 (2006) 14–21.
[9] Y. Jiang, S. Matsusaka, H. Masuda, Y. Qian, Development of measurement system for powder flowability based on vibrating capillary method, Powder Technol. 188 (2009) 242–247.
[10] T. Horio, M. Yasuda, S. Matsusaka, Measurement of flowability of lubricated powders by the vibrating tube method, Drug Dev. Ind. Pharm. 39 (2013) 1063–1069.
[11] I.M. Zainuddin, M. Yasuda, T. Horio, S. Matsusaka, Experimental study on powder flowability using vibration shear tube method, Part. Part. Syst. Char. 29 (2012) 8–15.
[12] T. Horio, M. Yasuda, S. Matsusaka, Effect of particle shape on powder flowability of microcrystalline cellulose as determined using the vibration shear tube method, Int. J. Pharm. 473 (2014) 572–578.
[13] J. Schwedes, Review on testers for measuring flow properties of bulk solids, Granul. Matt. 5 (2003) 1–43.
[14] K. Thalberg, D. Lindholm, A. Axelsson, Comparison of different flowability tests for powders for inhalation, Powder Technol. 146 (2004) 206–213.
[15] J.Y.S. Tay, C.V. Liew, P.W.S. Heng, Powder Flow Testing: judicious choice of test methods, AAPS Pharm. Sci. Tech. 18 (2017) 1843–1854.
[16] Y. Kudo, A. Uno, Y. Masatoshi, S. Matsusaka, Effect of surface modification with silicon compounds on flowability of granulated lactose, J. Soc. Powder Technol. Jpn. 54 (2017) 82–89.
[17] Y. Kudo, A. Uno, Y. Masatoshi, S. Matsusaka, Effect of addition ratio of silicic acid compounds on flowability of lactose, J. Soc. Powder Technol. Jpn. 54 (2017) 654–659.
[18] S. Jonat, S. Hasenzahl, M. Drechsler, P. Albers, K.G. Wagner, P.C. Schmidt, Investigation of compacted hydrophilic and hydrophobic colloidal silicon dioxides as glidants for pharmaceutical excipients, Powder Technol. 141 (2004) 31–43.
[19] H. Rumpf, Die wissenschaft des agglomerierens, Chem. Ing. Tech. 46 (1974) 1–11.
[20] Y.I. Rabinovich, J.J. Adler, A. Ata, R.K. Singh, B.M. Moudgil, Adhesion between nanoscale rough surfaces: I. Role of asperity geometry, J. Colloid Interf. Sci. 232 (2000) 10–16.
[21] Y.I. Rabinovich, J.J. Adler, A. Ata, R.K. Singh, B.M. Moudgil, Adhesion between nanoscale rough surfaces: II. Measurement and comparison with theory, J. Colloid Interf. Sci. 232 (2000) 17–24.
[22] X. Han, C. Ghoroi, D. To, Y. Chen, R. Davé, Simultaneous micronization and surface modification for improvement of flow and dissolution of drug particles, Int. J. Pharm. 415 (2011) 185–195.
[23] A.S. Persson, G. Alderborn, G. Frenning, Flowability of surface modified pharmaceutical granules: a comparative experimental and numerical study, Eur. J. Pharm. Biopharm. 42 (2011) 199–209.
[24] J. Vercruysse, D. Córdoba Díaz, E. Peeters, M. Fonteyne, U. Delaet, I. Van Assche, T. De Beer, J.P. Remon, C. Vervaet, Continuous twin screw granulation:

influence of process variables on granule and tablet quality, Eur. J. Pharm. Biopharm. 82 (2012) 205–211.
[25] W. Yu, K. Muteki, L. Zhang, G. Kim, Prediction of bulk powder flow performance using comprehensive particle size and particle shape distributions, J. Pharm. Sci. 100 (2011) 284–293.
[26] X. Fu, D. Huck, L. Makein, B. Armstrong, U. Willen, T. Freeman, Effect of particle shape and size on flow properties of lactose powders, Particuology 10 (2012) 203–208.
[27] F. Boschini, V. Delaval, K. Traina, N. Vandewalle, G. Lumay, Linking flowability and granulometry of lactose powders, Int. J. Pharm. 494 (2015) 312–320.
[28] Y. Takeuchi, T. Tomita, J. Kuroda, A. Kageyu, C. Yonekura, Y. Hiramura, K. Tahara, H. Takeuchi, Characterization of mannitol granules and powder: a comparative study using two flowability testers, Int. J. Pharm. 547 (2018) 106–113.
[29] H.P. Goh, P.W.S. Heng, C.V. Liew, Comparative evaluation of powder flow parameters with reference to particle size and shape, Int. J. Pharm. 547 (2018) 133–141.